

Blood

Supplementary information

Bruton's Tyrosine Kinase Degradation as a Therapeutic Strategy for Cancer

Dennis Dobrovolsky, Eric S. Wang, Sara Morrow, Catharine Leahy, Tyler Faust, Radosław P. Nowak, Katherine A. Donovan, Guang Yang, Zhengnian Li, Eric S. Fischer, Steven P. Treon, David M. Weinstock, and Nathanael S. Gray

Methods

Protein Docking. All protein docking was carried out using Rosetta 3.8 provided through SBGrid56. Input models were downloaded from the PDB (hsCRBN pdb: 5fqd, chain B; BTK pdb: 5P9J). Ligand conformers for lenalidomide were generated using OpenEye Omega (OpenEye scientific) and parameter files generated using Rosetta 'molfile_to_params.py'. hsCRBN bound lenalidomide and APO BTK coordinates were combined into a single file and prepared for docking using the Rosetta 'docking_prepack_protocol' program. Global docking was performed using Rosetta 'docking_protocol' with the following command line options:

- partners A_B - dock_pert 5 25 - randomize2 - ex1 ex2aro -nstruct 40000 -beta
providing the combined pdb and ligand specific parameter files as input.

To assess the landscape of possible binding modes for BTK, the top 200 lowest scoring docking decoys were selected, BTK was aligned to CGI1746-bound BTK (pdb: 3OCS) and the shortest pairwise distance between selected set of solvent accessible atoms on CGI1746 and set of atoms on lenalidomide was calculated in Pymol (The PyMOL Molecular Graphics System, Version 1.8.6.0 Schrödinger, LLC) as Euclidean distance for each of the top 200 poses and the shortest distance poses manually inspected and the shortest distance pose shown in Figure 1.

Sample preparation TMT LC-MS3 mass spectrometry. Mino cells were treated with DMSO or 200 nM of compounds DD-03-171, and DD-04-118 in biological triplicates for 4 hours and cells harvested by centrifugation. Lysis buffer (8 M Urea, 50 mM NaCl, 50 mM 4-(2hydroxyethyl)-1-piperazineethanesulfonic acid (EPPS) pH 8.5, Protease and Phosphatase inhibitors from Roche) was added to the cell pellets and homogenized by 20 passes through a 21 gauge (1.25 in. long) needle to achieve a cell lysate with a protein concentration between 1 – 4 mg mL⁻¹. A micro-BCA assay (Pierce) was used to determine the final protein concentration of protein in the cell lysate. 200 µg of protein for each sample were reduced and alkylated as previously described¹.

Proteins were precipitated using methanol/chloroform. In brief, four volumes of methanol were added to the cell lysate, followed by one volume of chloroform, and finally three volumes of water. The mixture was vortexed and centrifuged to separate the chloroform phase from the aqueous phase. The precipitated protein was washed with three volumes of methanol, centrifuged and the resulting washed precipitated protein was allowed to air dry. Precipitated protein was resuspended in 4 M Urea, 50 mM HEPES pH 7.4, followed by dilution to 1 M urea with the addition of 200 mM EPPS, pH 8. Proteins were first digested with LysC (1:50; enzyme:protein) for 12 hours at room temperature. The LysC digestion was diluted down to 0.5 M Urea with 200 mM EPPS pH 8 followed by digestion with trypsin (1:50; enzyme:protein) for 6 hours at 37 °C. Tandem mass tag (TMT) reagents (Thermo Fisher Scientific) were dissolved in anhydrous acetonitrile (ACN) according to manufacturer's instructions. Anhydrous ACN was added to each peptide sample to a final concentration of 30% v/v, and labeling was induced with the addition of TMT reagent to each sample at a ratio of 1:4 peptide:TMT label. The 10-plex labeling reactions were performed for 1.5 hours at room temperature and the reaction quenched by the addition of hydroxylamine to a final concentration of 0.3% for 15 minutes at room temperature. The sample channels were combined at a

1:1:1:1:1:1:1:1:1 ratio, desalted using C₁₈ solid phase extraction cartridges (Waters) and analyzed by LC-MS for channel ratio comparison. Samples were then combined using the adjusted volumes determined in the channel ratio analysis and dried down in a speed vacuum. The combined sample was then resuspended in 1% formic acid, and acidified (pH 2–3) before being subjected to desalting with C₁₈ SPE (Sep-Pak, Waters). Samples were then offline fractionated into 96 fractions by high pH reverse-phase HPLC (Agilent LC1260) through an aeris peptide xb-c18 column (phenomenex) with mobile phase A containing 5% acetonitrile and 10 mM NH₄HCO₃ in LC-MS grade H₂O, and mobile phase B containing 90% acetonitrile and 10 mM NH₄HCO₃ in LC-MS grade H₂O (both pH 8.0). The 96 resulting fractions were then pooled in a non-continuous manner into 24 fractions and these fractions were used for subsequent mass spectrometry analysis.

Data were collected using an Orbitrap Fusion Lumos mass spectrometer (Thermo Fisher Scientific, San Jose, CA, USA) coupled with a Proxeon EASY-nLC 1200 LC pump (Thermo Fisher Scientific). Peptides were separated on a 75 μM inner diameter microcapillary column packed with ~ 50 cm of Accucore C18 resin (2.6 μM, 100 Å, ThermoFisher Scientific). Peptides were separated using a 190 min gradient of 6 – 27% acetonitrile in 1% formic acid with a flow rate of 450 nL min⁻¹.

Each analysis used an MS³-based TMT method as described previously². The data were acquired using a mass range of *m/z* 340 – 1350, resolution 120,000, AGC target 1 x 10⁶, maximum injection time 100 ms, dynamic exclusion of 120 seconds for the peptide measurements in the Orbitrap. Data dependent MS² spectra were acquired in the ion trap with a normalized collision energy (NCE) set at 35%, AGC target set to 1.8 x 10⁴ and a maximum injection time of 120 ms. MS³ scans were acquired in the Orbitrap with a HCD collision energy set to 55%, AGC target set to 1.5 x 10⁵, maximum injection time of 150 ms, resolution at 50,000 and with a maximum synchronous precursor selection (SPS) precursors set to 10. The Advanced Peak Detection (APD) algorithm was disabled.

Patient-Derived Xenograft Models.

The PDX model DFBL-18689 was injected into 15 NSG mice (1x10⁶ cells per mouse) via tail vein injection. When the mice reached an average of 0.4% hCD19/hCD20+ circulating disease by flow cytometry, they were dosed with vehicle (5% DMSO, 10% (2-hydroxypropyl)-β-cyclodextrin [HP-β-CD] in PBS daily IP; sterile water via oral gavage [OG] daily), ibrutinib (30mpk OG daily), lenalidomide (50mpk IP daily), combined lenalidomide (50mpk IP daily) and ibrutinib (30mpk via OG daily), or DD-03-171 (50mpk IP daily).

The PDX model DFBL-39435 was injected into 9 NSG mice (1x10⁶ cells per mouse) via tail vein injection. When the mice reached an average of 0.6% hCD45/hCD20+ circulating disease by flow cytometry, they were dosed with vehicle (5% DMSO, 10% HP-β-CD in PBS daily IP; sterile water via OG daily), combined lenalidomide (50mpk IP daily) and ibrutinib (30mpk via OG daily), or DD-03-171 (50mpk IP daily) and were sacrificed on treatment day 14. One mouse in the vehicle cohort did not engraft (below 0.1% hCD45/hCD20+ on treatment day 1) and was excluded from the study.

The PDX model DFBL-44685 was injected into 32 NSG mice (1×10^6 cells per mouse) via tail vein injection. When mice reached an average of 0.74% (survival cohort) or 1.5% (pharmacodynamic [PD] cohort) hCD19/hCD45+ circulating disease by flow cytometry, they were split into PD (n=3/arm) and survival (n=5/arm) treatment groups and dosed with vehicle (5% DMSO, 10% HP- β -CD in PBS daily IP), ibrutinib (30mpk via OG daily), lenalidomide (50mpk IP daily) or DD-03-171 (50mpk IP daily). Mice in the PD arms were sacrificed on treatment day 3; the survival arms received ongoing treatment and were sacrificed when they required sacrifice based on the Dana-Farber Cancer Institute's Institutional Animal Care and Use Committee (IACUC)-approved protocol.

The PDX model DFBL-96069 was injected into 32 NSG mice (1×10^6 cells per mouse) via tail vein injection. When mice reached an average of 2% (survival cohort) or 5% (pharmacodynamic [PD] cohort) hCD19/hCD45+ circulating disease by flow cytometry, they were split into PD (n=3/arm) and survival (n=5/arm) treatment groups and dosed with vehicle (5% DMSO, 10% HP- β -CD in PBS daily IP), ibrutinib (30mpk via OG daily), lenalidomide (50mpk IP daily) or DD-03-171 (50mpk IP daily). Mice in the PD arms were sacrificed on treatment day 3; the survival arms received ongoing treatment and were sacrificed when they became clinically ill. Three mice from the ibrutinib cohort and one mouse from the lenalidomide cohort were euthanized in accordance with the IACUC-approved protocol due to infections unrelated to the tumor, and were censored from this study.

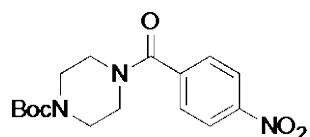
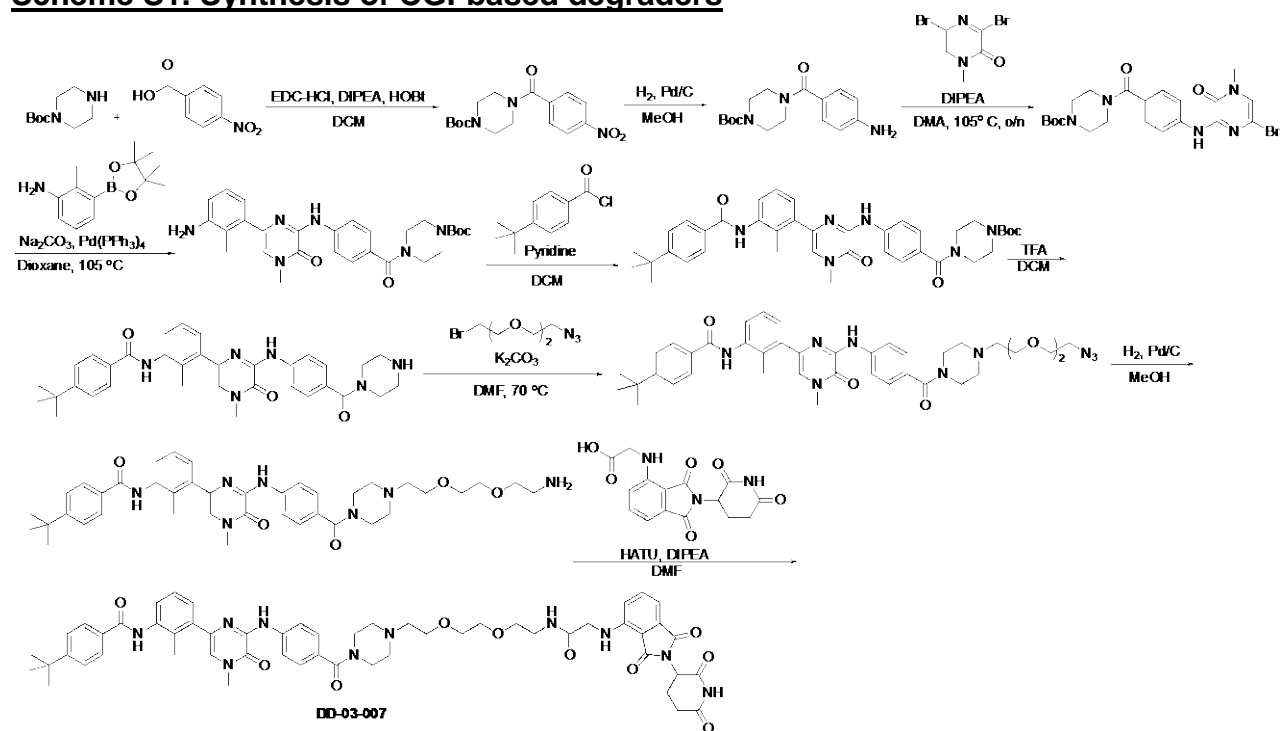
The luciferized PDX model DFBL-98848 was injected into 15 NSG mice (1×10^6 cells per mouse) via tail vein injection. When the mice reached an average of 3×10^8 ph/s/cm²/sr bioluminescence, they were dosed with vehicle (5% DMSO, 10% HP- β -CD in PBS daily IP; sterile water via OG daily), ibrutinib (30mpk OG daily), lenalidomide (50mpk IP daily), combined lenalidomide (50mpk IP daily) and ibrutinib (30mpk via OG daily), or DD-03-171 (50mpk IP daily) and were sacrificed when they became clinically ill, up until the combination group required sacrifice based on IACUC criteria, upon which all remaining mice were sacrificed. Three injected mice were excluded and did not receive treatment due to insufficient engraftment (less than 1×10^6 ph/s/cm²/sr). One mouse from the ibrutinib cohort was euthanized in accordance with the IACUC protocol due to trauma from a submandibular bleed and was censored from this study.

Peripheral blood and spleens were harvested. Circulating and splenic disease burden were measured via flow cytometry (CD19-V450, Cat # 560353, BD Horizon; CD45-APC, Cat # 17-0459-42, Invitrogen), and complete blood counts were collected using a HEMAvet 950 (Drew Scientific, CDC-9950-002). Splenic lymphoma cells were mouse cell-depleted (Stemcell EasySep Mouse/Human Chimera Isolation Kit, Cat # 19849A) and viably frozen.

Chemical synthesis. Commercially available reagents and solvents were used without further purification. All reactions were monitored by thin layer chromatography (TLC) with 0.25 mm E. Merck pre-coated silica gel plates (60 F254) and/or Waters LCMS system (Waters 2489 UV/Visible Detector, Waters 3100 Mass, Waters 515 HPLC pump,

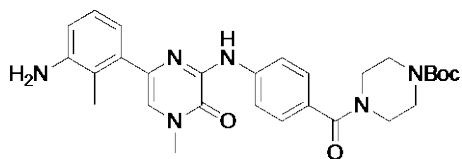
Waters 2545 Binary Gradient Module, Waters Reagent Manager, Waters 2767 Sample Manager) using SunFire™ C18 column (4.6 x 50 mm, 5 μm particle size): solvent A = 0.035% TFA in Water; solvent B = 0.035% TFA in MeOH; flow rate: 2.5 ml min⁻¹. Purification of reaction products was carried out by flash chromatography using CombiFlash®Rf with Teledyne Isco RediSep®Rf High Performance Gold or Silicycle SiliaSep™ High Performance columns (4 g, 12 g or 24 g) and Waters LCMS system using SunFire™ Prep C18 column (19 x 50 mm, 5 μm particle size): solvent A = 0.035% TFA in Water; solvent B = 0.035% TFA in MeOH; flow rate: 25 ml min⁻¹. The purity of all compounds was over 95% and was analyzed with Waters LCMS system. ¹H NMR spectra and ¹³C NMR spectra were obtained using a Bruker 500 (500 MHz for ¹H NMR and 125 MHz for ¹³C NMR). Chemical shifts are reported relative to dimethyl sulfoxide (δ = 2.50) for ¹H and dimethyl sulfoxide (δ = 39.51) for ¹³C NMR. Data are reported as (bs = broad singlet, s = singlet, d = doublet, t = triplet, q = quartet, m = multiplet).

Scheme S1. Synthesis of CGI-based degraders

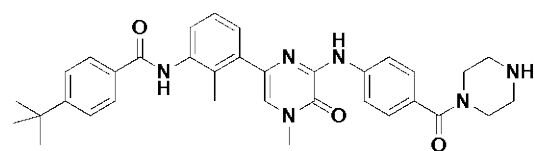


Tert-butyl 4-(4-nitrobenzoyl)piperazine-1-carboxylate. To a solution of tert-butyl piperazine-1-carboxylate (3.1 g, 16.6 mmol, 1 equiv.), 4-nitrobenzoic acid (2.8 g, 16.6 mmol, 1 equiv.), N,N-diisopropylethylamine (5.8 mL, 33.2 mmol, 2 equiv.), and hydroxybenzotriazole (2.2 g, 16.6 mmol, 1 equiv.) in anhydrous DCM (40 mL) was added N-(3-dimethylaminopropyl)-N'-ethylcarbodiimide hydrochloride (3.8 g, 20.0 mmol,

1.2 equiv.) at 0° C. The solution was warmed to room temperature and stirred for 24h. Water was added and the mixture was extracted 3x with DCM. The combined organic layers were dried with Na₂SO₄, filtered, and concentrated, then purified *via* silica gel column chromatography to obtain the product as a yellow solid (4.6 g, 13.7 mmol, 82% yield). MS (ESI) m/z 336 (M+H)⁺.

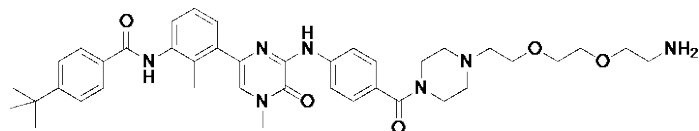


Tert-butyl 4-(4-((6-(3-amino-2-methylphenyl)-4-methyl-3-oxo-3,4-dihydropyrazin-2-yl)amino)benzoyl)piperazine-1-carboxylate. A solution of tert-butyl 4-(4-aminobenzoyl)piperazine-1-carboxylate (1.7 g, 5.7 mmol, 1 equiv.), 3,5-dibromo-1-methylpyrazin-2(1H)-one (1.8 g, 6.8 mmol, 1.2 equiv.) and N,N-diisopropylethylamine (1.48 mL, 8.5 mmol, 1.5 equiv.) in N,N-dimethylacetamide (5 mL) was stirred in a sealed vial at 105 °C for 30h. The reaction was cooled to room temperature then EtOAc (20 mL) was added. The solid precipitate was filtered and dried on high vacuum overnight to obtain the crude intermediate tert-butyl 4-(4-((6-bromo-4-methyl-3-oxo-3,4-dihydropyrazin-2-yl)amino)benzoyl)piperazine-1-carboxylate. This compound (1 g, 2.0 mmol, 1 equiv.) was dissolved in anhydrous 1,4-dioxane (6 mL) and to the solution was added Na₂CO₃ (323 mg, 3.0 mmol, 1.5 equiv.) and H₂O (1.2 mL). The mixture was degassed by bubbling N₂ (g) through it for 10 min. Pd(PPh₃)₄ (328 mg, 0.28 mmol, 0.14 equiv.) was added, the vial was sealed, then stirred at 105 °C for 16h. The reaction was cooled to r.t. and filtered through Celite. The filtrate was concentrated then the residue was redissolved in EtOAc and washed 1x with saturated NaHCO_{3(aq)}. The organic layer was dried with Na₂SO₄, filtered, then concentrated. The residue was purified *via* silica gel column chromatography to obtain the product as a white solid (244 mg, 0.47 mmol, 27% yield). MS (ESI) m/z 520 (M+H)⁺.

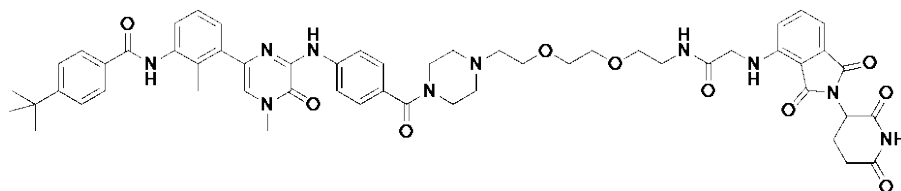


4-(tert-butyl)-N-(2-methyl-3-(4-methyl-5-oxo-6-((4-(piperazine-1-carbonyl)phenyl)amino)-4,5-dihydropyrazin-2-yl)phenyl)benzamide. To a solution of tert-butyl 4-(4-((6-(3-amino-2-methylphenyl)-4-methyl-3-oxo-3,4-dihydropyrazin-2-yl)amino)benzoyl)piperazine-1-carboxylate (238 mg, 0.46 mmol, 1 equiv.) in anhydrous DCM (4 mL) was added anhydrous pyridine (56 µL, 0.68 mmol, 1.5 equiv.) and 4-*tert*-butyl benzoyl chloride (107 µL, 0.55 mmol, 1.2 equiv.). After stirring at room temperature for 1h, the reaction was concentrated to obtain a crude solid, which was subjected to the next step directly. The crude solid was dissolved in anhydrous DCM (3 mL), then trifluoroacetic acid (3 mL) was added. After stirring for 2h, the reaction was concentrated, redissolved in DMSO, then purified using an HPLC with a reverse phase C18 column to afford the product as a white solid (154 mg, 0.22 mmol, 48% yield over two steps). ¹H NMR (500 MHz, DMSO-*d*₆) δ 9.90 (s, 1H), 9.50 (s, 1H), 8.85 (s, 2H), 8.11 (d, *J* = 8.7 Hz, 2H), 7.95

(d, $J = 8.4$ Hz, 2H), 7.55 (d, $J = 8.5$ Hz, 2H), 7.42 – 7.34 (m, 3H), 7.33 – 7.27 (m, 3H), 3.67 (bs, 4H), 3.57 (s, 3H), 3.17 (bs, 4H), 2.28 (s, 3H), 1.33 (s, 9H). MS (ESI) m/z 580 ($M+H$)⁺.



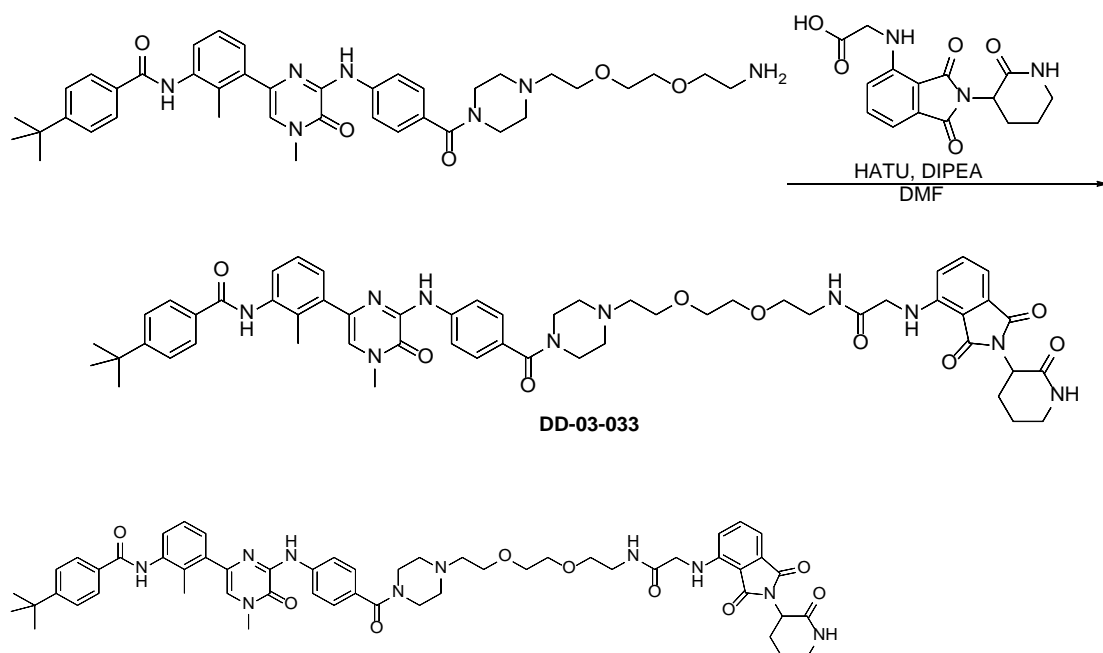
N-(3-(6-((4-(4-(2-(2-(2-aminoethoxy)ethoxy)ethyl)piperazine-1-carbonyl)phenyl)amino)-4-methyl-5-oxo-4,5-dihydropyrazin-2-yl)-2-methylphenyl)-4-(tert-butyl)benzamide. 4-(tert-butyl)-*N*-(2-methyl-3-(4-methyl-5-oxo-6-((4-(piperazine-1-carbonyl)phenyl)amino)-4,5-dihydropyrazin-2-yl)phenyl)benzamide (94 mg, 0.163 mmol, 1 equiv.), tert-butyl (2-(2-(2-bromoethoxy)ethoxy)ethyl)carbamate (111 mg, 0.356 mmol, 2 equiv.), and K_2CO_3 (113 mg, 0.815 mmol, 5 equiv.) were dissolved in anhydrous DMF (2 mL) and stirred at 80 °C in a sealed vial for 8h. The reaction was cooled to room temperature and water (3 mL) was added. The reaction was extracted with EtOAc (4x 10 mL). The combined organic layers were further washed with H_2O (2x 3 mL) and brine (1x 3 mL), then dried with Na_2SO_4 , filtered, and concentrated to afford a crude oil. The crude oil was dissolved in anhydrous DCM (2 mL), then trifluoroacetic acid (2 mL) was added and the reaction was stirred for 20 min. The solution was concentrated then purified using an HPLC with a reverse phase C18 column to afford the product as a white solid (16 mg, 0.02 mmol, 12% yield over two steps). 1H NMR (500 MHz, $DMSO-d_6$) δ 9.91 (s, $J = 8.0$ Hz, 1H), 9.51 (s, $J = 18.5$ Hz, 1H), 8.12 (d, $J = 8.7$ Hz, 2H), 7.95 (d, $J = 8.5$ Hz, 2H), 7.84 (s, $J = 18.4$ Hz, 3H), 7.58 – 7.51 (m, 2H), 7.43 – 7.33 (m, 3H), 7.33 – 7.23 (m, 3H), 3.82 – 3.68 (m, 2H), 3.65 – 3.52 (m, 10H), 3.40 – 3.23 (m, 7H), 3.19 – 3.04 (m, 2H), 3.04 – 2.87 (m, 2H), 2.29 (s, 3H), 1.33 (s, 9H). MS (ESI) m/z 711 ($M+H$)⁺.



4-(tert-butyl)-*N*-(3-(6-((4-(4-(2-(2-(2-((2-(2,6-dioxopiperidin-3-yl)-1,3-dioxoisindolin-4-yl)amino)acetamido)ethoxy)ethoxy)ethyl)piperazine-1-carbonyl)phenyl)amino)-4-methyl-5-oxo-4,5-dihydropyrazin-2-yl)-2-methylphenyl)benzamide (**DD-03-007**). To a solution of *N*-(3-(6-((4-(4-(2-(2-(2-aminoethoxy)ethoxy)ethyl)piperazine-1-carbonyl)phenyl)amino)-4-methyl-5-oxo-4,5-dihydropyrazin-2-yl)-2-methylphenyl)-4-(tert-butyl)benzamide trifluoroacetic acid salt (8 mg, 0.0815 mmol), (2-(2,6-dioxopiperidin-3-yl)-1,3-dioxoisindolin-4-yl)glycine (40 mg, 0.122 mmol, 1.5 equiv.), and diisopropylethylamine (43 μ L, 0.244 mmol, 3 equiv.) in anhydrous DMF (1 mL) was added 1-[Bis(dimethylamino)methylene]-1H-1,2,3-triazolo[4,5-b]pyridinium 3-oxid hexafluorophosphate (50 mg, 0.130 mmol, 1.6 equiv.) and stirred at r.t. for 1h. The reaction was purified using an HPLC with a reverse phase C18 column then further purified *via* silica gel column chromatography (0 – 10% MeOH (with 1.75N NH_3) in DCM) to obtain the product as a yellow solid (9.4 mg, 0.0092 mmol, 11% yield). 1H NMR

(500 MHz, DMSO-*d*₆) δ 11.09 (s, 1H), 9.88 (s, 1H), 9.44 (s, 1H), 8.14 (t, *J* = 5.4 Hz, 1H), 8.07 (d, *J* = 8.3 Hz, 2H), 7.94 (d, *J* = 8.4 Hz, 2H), 7.56 (dd, *J* = 18.7, 8.0 Hz, 3H), 7.42 – 7.20 (m, 6H), 7.06 (d, *J* = 7.0 Hz, 1H), 6.94 (t, *J* = 5.6 Hz, 1H), 6.85 (d, *J* = 8.5 Hz, 1H), 5.07 (dd, *J* = 12.7, 5.3 Hz, 1H), 3.92 (d, *J* = 5.5 Hz, 2H), 3.69 – 3.36 (m, 16H), 3.28 – 3.19 (m, 2H), 2.89 (dd, *J* = 21.4, 9.5 Hz, 1H), 2.56 (dd, *J* = 26.9, 13.2 Hz, 3H), 2.41 (s, 4H), 2.28 (s, 3H), 2.09 – 1.96 (m, 1H), 1.32 (s, 9H). ¹³C NMR (126 MHz, DMSO-*d*₆) δ 172.80, 170.03, 168.85, 168.69, 168.56, 167.30, 165.30, 154.41, 150.41, 146.26, 145.80, 141.18, 138.25, 137.16, 136.19, 132.52, 132.04, 131.79, 131.11, 128.94, 127.83, 127.52, 127.13, 126.51, 125.46, 125.20, 120.48, 118.51, 117.44, 110.97, 109.85, 91.52, 69.59, 69.51, 68.93, 68.18, 57.02, 53.15, 48.57, 45.16, 39.52, 36.60, 34.67, 30.98, 30.95, 22.16, 15.56. MS (ESI) *m/z* 1024 (M+H)⁺.

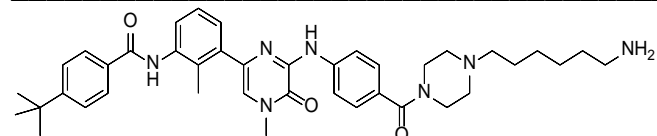
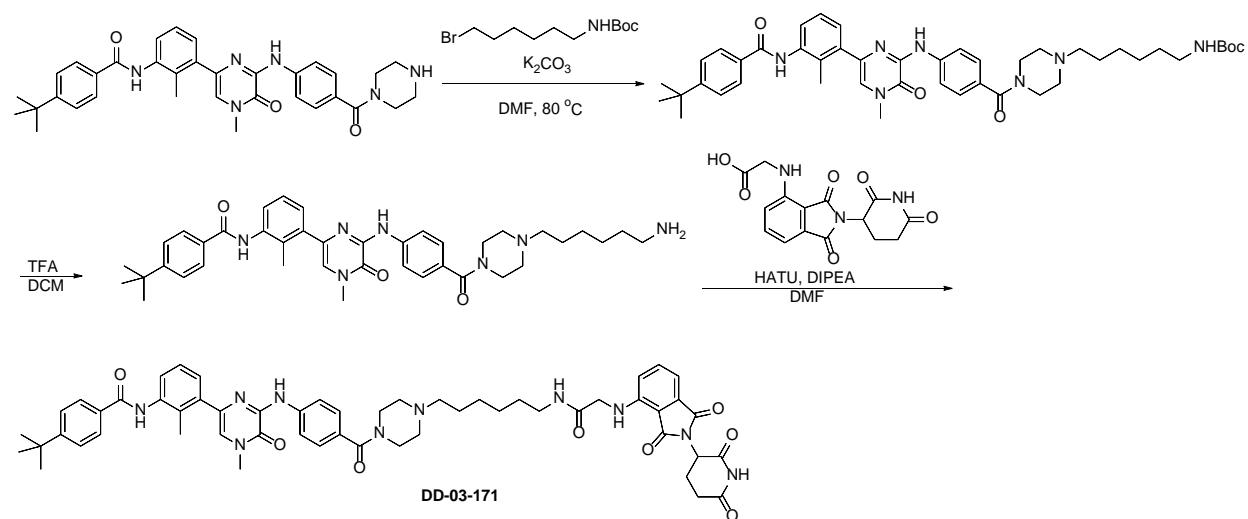
Scheme S2. Synthesis of DD-03-033



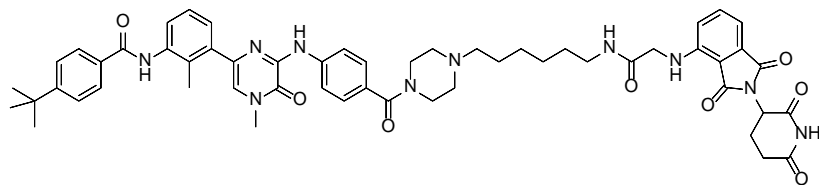
4-(tert-butyl)-N-(3-(6-((4-(4-(2-(2-(2-((1,3-dioxo-2-(2-oxopiperidin-3-yl)isoindolin-4-yl)amino)acetamido)ethoxy)ethoxy)ethyl)piperazine-1-carbonyl)phenyl)amino)-4-methyl-5-oxo-4,5-dihydropyrazin-2-yl)-2-methylphenyl)benzamide (DD-03-033). To a solution of N-(3-(6-((4-(4-(2-(2-(2-aminoethoxy)ethoxy)ethyl)piperazine-1-carbonyl)phenyl)amino)-4-methyl-5-oxo-4,5-dihydropyrazin-2-yl)-2-methylphenyl)-4-(tert-butyl)benzamide (common intermediate – see Scheme S1; 62 mg, 0.088 mmol, 1 equiv.), (1,3-dioxo-2-(2-oxopiperidin-3-yl)isoindolin-4-yl)glycine (28 mg, 0.088 mmol, 1 equiv.), and diisopropylethylamine (46 μL, 0.264 mmol, 3 equiv.) in anhydrous DMF (1 mL) was added 1-[Bis(dimethylamino)methylene]-1H-1,2,3-triazolo[4,5-b]pyridinium 3-oxid hexafluorophosphate (44 mg, 0.114 mmol, 1.3 equiv.) and stirred at r.t. for 1h. The reaction was purified using an HPLC with a reverse phase C18 column to obtain the product as a yellow solid (6.8 mg, 0.0067 mmol, 8% yield). ¹H NMR (500 MHz, DMSO-*d*₆) δ 9.88 (s, 1H), 9.43 (s, 1H), 8.13 (t, *J* = 5.6 Hz, 1H), 8.07 (d, *J* = 8.3 Hz, 2H), 7.94 (d, *J* = 8.0 Hz, 2H), 7.81 (s, 1H), 7.55 (t, *J* = 7.4 Hz, 3H), 7.44 – 7.35 (m, 1H), 7.35 – 7.18

(m, 5H), 7.03 (d, $J = 7.1$ Hz, 1H), 6.92 (t, $J = 5.7$ Hz, 1H), 6.82 (d, $J = 8.5$ Hz, 1H), 4.52 (dd, $J = 11.9, 6.3$ Hz, 1H), 3.91 (d, $J = 5.6$ Hz, 2H), 3.68 – 3.38 (m, 15H), 3.28 – 3.12 (m, 3H), 2.60 – 2.34 (m, 8H), 2.34 – 2.13 (m, 4H), 2.05 – 1.72 (m, 2H), 1.32 (s, 9H). ^{13}C NMR (126 MHz, $\text{DMSO-}d_6$) δ 169.06, 168.88, 168.62, 167.56, 167.14, 165.34, 154.44, 150.43, 148.38, 146.28, 145.65, 141.18, 138.27, 137.18, 136.01, 132.54, 132.26, 131.80, 131.14, 128.96, 127.84, 127.53, 127.15, 126.53, 125.48, 125.22, 120.50, 118.53, 117.19, 110.77, 110.17, 69.61, 69.53, 68.94, 68.20, 57.04, 48.61, 45.21, 41.43, 38.66, 36.63, 34.69, 30.96, 25.92, 21.76, 15.58. MS (ESI) m/z 1010 ($\text{M}+\text{H}$) $^+$.

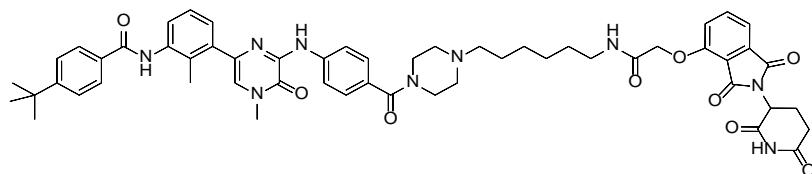
Scheme S3. Synthesis of DD-03-171



N-(3-(6-((4-(4-(6-aminohexyl)piperazine-1-carbonyl)phenyl)amino)-4-methyl-5-oxo-4,5-dihydropyrazin-2-yl)-2-methylphenyl)-4-(tert-butyl)benzamide. 4-(tert-butyl)-*N*-(2-methyl-3-(4-methyl-5-oxo-6-((4-(piperazine-1-carbonyl)phenyl)amino)-4,5-dihydropyrazin-2-yl)phenyl)benzamide (common intermediate – see Scheme S1; 151 mg, 0.2 mmol, 1 equiv.), tert-butyl (6-bromohexyl)carbamate (112 mg, 0.4 mmol, 2 equiv.), and K_2CO_3 (138 mg, 1.0 mmol, 5 equiv.) were dissolved in anhydrous DMF (1 mL) and stirred at 80 °C in a sealed vial for 5h. The reaction was cooled to room temperature and water (3 mL) was added. The reaction was extracted with EtOAc (4x 10 mL). The combined organic layers were further washed with H_2O (2x 3 mL) and brine (1x 3 mL), then dried with Na_2SO_4 , filtered, and concentrated to afford a crude oil. The crude oil was dissolved in DCM (2 mL) and TFA (2 mL) then stirred for 30 min. The solution was concentrated then purified using an HPLC with a reverse phase C18 column to afford the product as a clear oil (68 mg, 0.1 mmol, 50% yield over two steps). MS (ESI) m/z 755 ($\text{M}+\text{H}$) $^+$.



4-(tert-butyl)-N-(3-(6-((4-(4-(6-(2-((2-(2,6-dioxopiperidin-3-yl)-1,3-dioxoisindolin-4-yl)amino)acetamido)hexyl)piperazine-1-carbonyl)phenyl)amino)-4-methyl-5-oxo-4,5-dihydropyrazin-2-yl)-2-methylphenyl)benzamide (DD-03-171). To a solution of *N-(3-(6-((4-(4-(6-amino)hexyl)piperazine-1-carbonyl)phenyl)amino)-4-methyl-5-oxo-4,5-dihydropyrazin-2-yl)-2-methylphenyl)-4-(tert-butyl)benzamide* (75 mg, 0.1 mmol, 1 equiv.), *(2-(2,6-dioxopiperidin-3-yl)-1,3-dioxoisindolin-4-yl)glycine* (33 mg, 0.1 mmol, 1. equiv.), and diisopropylethylamine (87 μ L, 0.5 mmol, 5 equiv.) in anhydrous DMF (1 mL) was added 1-[Bis(dimethylamino)methylene]-1H-1,2,3-triazolo[4,5-b]pyridinium 3-oxid hexafluorophosphate (49 mg, 0.13 mmol, 1.3 equiv.) and stirred at r.t. for 1h. The reaction was purified using an HPLC with a reverse phase C18 column to obtain the product as a yellow solid (9.9 mg, 0.01 mmol, 10% yield). ^1H NMR (500 MHz, $\text{DMSO-}d_6$) δ 11.10 (s, 1H), 9.96 (s, 1H), 9.90 (s, 1H), 9.50 (s, 1H), 8.18 – 8.06 (m, 2H), 7.99 – 7.89 (m, 2H), 7.64 – 7.51 (m, 3H), 7.44 – 7.34 (m, 3H), 7.34 – 7.25 (m, 3H), 7.08 (d, J = 7.1 Hz, 1H), 6.94 (s, 1H), 6.85 (d, J = 8.6 Hz, 1H), 5.07 (dd, J = 12.7, 5.4 Hz, 1H), 3.92 (d, J = 4.6 Hz, 2H), 3.46 (s, 2H), 3.31 (s, 4H), 3.14 – 2.96 (m, 6H), 2.95 – 2.82 (m, 1H), 2.66 – 2.53 (m, 2H), 2.28 (s, 3H), 2.09 – 1.92 (m, 1H), 1.61 (s, 2H), 1.40 (d, J = 6.9 Hz, 2H), 1.32 (s, 9H), 1.31 – 1.18 (m, 6H). ^{13}C NMR (126 MHz, DMSO) δ 172.87, 170.10, 169.19, 168.76, 168.35, 167.37, 165.41, 154.51, 150.47, 146.29, 145.84, 141.84, 138.28, 137.19, 136.25, 132.63, 132.10, 131.80, 131.10, 128.27, 127.57, 127.48, 127.25, 126.64, 125.54, 125.25, 118.53, 117.47, 111.05, 109.91, 55.63, 50.72, 48.62, 45.22, 38.41, 36.68, 34.71, 31.02, 30.98, 28.81, 25.79, 25.62, 23.09, 22.20, 15.56. MS (ESI) m/z 992 ($\text{M}+\text{H}$) $^+$.



4-(tert-butyl)-N-(3-(6-((4-(4-(6-(2-((2-(2,6-dioxopiperidin-3-yl)-1,3-dioxoisindolin-4-yl)oxy)acetamido)hexyl)piperazine-1-carbonyl)phenyl)amino)-4-methyl-5-oxo-4,5-dihydropyrazin-2-yl)-2-methylphenyl)benzamide (DD-04-118). To a solution of *N-(3-(6-((4-(4-(6-amino)hexyl)piperazine-1-carbonyl)phenyl)amino)-4-methyl-5-oxo-4,5-dihydropyrazin-2-yl)-2-methylphenyl)-4-(tert-butyl)benzamide* (75 mg, 0.1 mmol, 1 equiv.), *2-((2-(2,6-dioxopiperidin-3-yl)-1,3-dioxoisindolin-4-yl)oxy)acetic acid* (33 mg, 0.1 mmol, 1. equiv.), and diisopropylethylamine (87 μ L, 0.5 mmol, 5 equiv.) in anhydrous DMF (1 mL) was added 1-[Bis(dimethylamino)methylene]-1H-1,2,3-triazolo[4,5-b]pyridinium 3-oxid hexafluorophosphate (49 mg, 0.13 mmol, 1.3 equiv.) and stirred at r.t. for 1h. The reaction was purified using an HPLC with a reverse phase C18 column to obtain the product as a yellow solid (9.9 mg, 0.01 mmol, 10% yield). ^1H NMR (500 MHz, $\text{DMSO-}d_6$) δ 11.11 (s, 1H), 9.90 (s, 1H), 9.69 (s, 1H), 9.51 (s, 1H), 8.12 (d, J = 8.7 Hz, 2H), 8.02 – 7.89 (m, 3H), 7.81 (dd, J = 8.5, 7.3 Hz, 1H), 7.60 – 7.46 (m,

3H), 7.46 – 7.34 (m, 4H), 7.34 – 7.21 (m, 3H), 5.11 (dd, J = 12.9, 5.4 Hz, 1H), 4.77 (s, 2H), 3.57 (s, 4H), 3.28 (s, 1H), 3.15 (q, J = 6.7 Hz, 2H), 3.06 (s, 4H), 2.89 (ddd, J = 17.0, 13.9, 5.3 Hz, 1H), 2.58 (d, J = 37.4 Hz, 2H), 2.28 (s, 3H), 2.09 – 1.95 (m, 1H), 1.60 (s, 2H), 1.44 (d, J = 10.0 Hz, 2H), 1.32 (s, 9H), 1.31 – 1.13 (m, 6H). ¹³C NMR (126 MHz, DMSO-*d*₆) δ 172.78, 169.87, 169.10, 166.71, 166.68, 165.52, 165.31, 155.04, 154.43, 150.41, 146.25, 141.83, 138.24, 137.15, 136.93, 133.04, 132.56, 131.78, 131.02, 128.23, 127.51, 127.41, 127.18, 126.57, 125.47, 125.19, 120.68, 120.42, 118.47, 116.83, 116.10, 67.68, 55.58, 50.71, 48.80, 39.52, 38.13, 36.62, 34.67, 30.94, 28.73, 25.71, 25.55, 23.07, 21.98, 15.51. MS (ESI) m/z 993 (M+H)⁺.

Tables

Table S1. Degree of kinase inhibition according to FRET-based Z'-Lyte technology assay (Invitrogen).

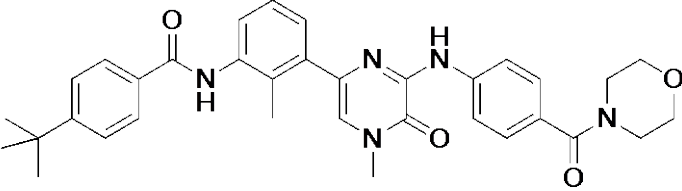
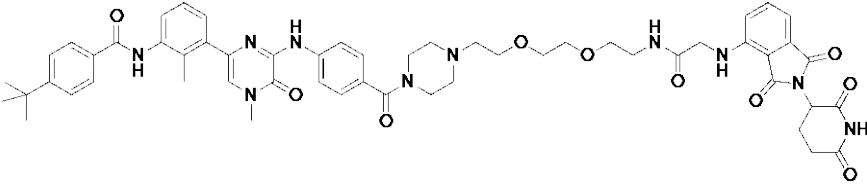
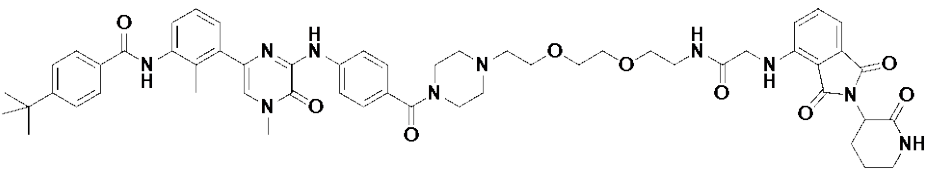
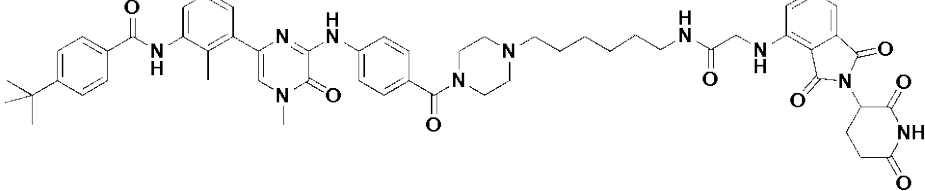
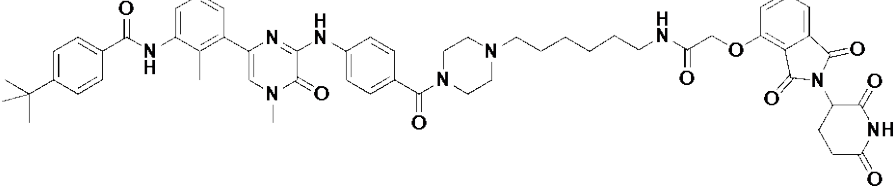
Name	Structure	BTK IC ₅₀ (nM)
CGI1746		1.9
DD-03-007		5.62
DD-03-033		5.65
DD-03-171		11.7
DD-04-118		4.13

Table S2. Pharmacokinetic data for DD-03-007

Formulation concentrations: 0.2mg/mL solution (2 mg/kg IV), 1mg/ml solution (10 mk/kg IP and PO), 2.5mg/mL solution (25mg/Kg PO), 5mg/ml suspension (50mg/Kg IP+PO)											
2 mg/kg IV											
Subject	T _{1/2} hr	T _{max} hr	C _{max} ng/mL	C _{max} µM	AUC _{last} min*ng/mL	AUC _{last} µM.hr	AUC _{INF_obs} min*ng/mL	AUC %Extrap	Cl _{obs} mL/min/kg	MRT _{INF_obs} hr	Vss _{obs} L/kg
2 mg/kg IV Mouse-1	1.60	0.08	3920	3.83	122827	2.00	123478	0.53	16.20	0.57	0.55
2 mg/kg IV Mouse-2	1.81	0.08	1510	1.48	31636	0.52	31965	1.03	62.57	0.60	2.27
2 mg/kg IV Mouse-3	2.15	0.08	2880	2.81	59340	0.97	59992	1.09	33.34	0.52	1.04
Avg.	1.85	0.08	2770	2.71	71268	1.16	71812	0.88	37.37	0.56	1.29
10 mg/kg IP											
Subject	T _{1/2} hr	T _{max} hr	C _{max} ng/mL	C _{max} µM	AUC _{last} min*ng/mL	AUC _{last} µM.hr	AUC _{INF_obs} min*ng/mL	AUC %Extrap	Cl _{obs} mL/min/kg	%F	Cl/%F
10 mg/kg IP Mouse-4	2.51	0.25	291	0.28	12702	0.21	13050	2.67	766.28		
10 mg/kg IP Mouse-5	1.07	0.50	2870	2.80	220617	3.59	221724	0.50	45.10		
10 mg/kg IP Mouse-6	1.08	0.50	3900	3.81	302280	4.92	303371	0.36	32.96		
Avg.	1.56	0.42	2354	2.30	178533	2.91	179382	1.18	281.45	50.1%	

Table S3. Pharmacokinetic data for DD-03-171

Formulation concentrations: 0.2mg/mL solution (2 mg/kg IV), 1mg/ml solution (10 mk/kg IP and PO), 2.5mg/mL solution (25mg/Kg PO), 5mg/ml suspension (50mg/Kg IP+PO)											
2 mg/kg IV											
Subject	T _{1/2} hr	T _{max} hr	C _{max} ng/mL	C _{max} µM	AUC _{last} min*ng/mL	AUC _{last} µM.hr	AUC _{INF_obs} min*ng/mL	AUC %Extrap	Cl _{obs} mL/min/kg	MRT _{INF_obs} hr	Vss _{obs} L/kg
2 mg/kg IV Mouse-1	1.99	0.08	507	0.51	37761	0.64	39764	5.0	50	2.4	7.3
2 mg/kg IV Mouse-2	1.57	0.08	1530	1.54	77161	1.30	79332	2.7	25	1.0	1.5
2 mg/kg IV Mouse-3	1.37	0.08	556	0.56	37065	0.62	38608	4.0	52	1.8	5.6
Avg.	1.64	0.08	864	0.87	50662	0.85	52568	3.9	42	1.8	4.8
10 mg/kg IP											
Subject	T _{1/2} hr	T _{max} hr	C _{max} ng/mL	C _{max} µM	AUC _{last} min*ng/mL	AUC _{last} µM.hr	AUC _{INF_obs} min*ng/mL	AUC %Extrap	Cl _{obs} mL/min/kg	%F	Cl/%F
10 mg/kg IP Mouse-4	1.22	0.50	197	0.20	22717	0.38	23308	2.5	429		48

10 mg/kg IP Mouse-5	2.72	0.25	191	0.19	31686	0.53	41374	23.4	242		27
10 mg/kg IP Mouse-6	2.89	0.50	212	0.21	30253	0.51	40050	24.5	250		28
Avg.	2.28	0.42	200	0.20	28219	0.47	34911	16.8	307	0.11	34
Subject	T_{1/2} hr	T_{max} hr	C_{max} ng/mL	C_{max} μM	AUC_{last} min*ng/mL	AUC_{last} μM.hr	AUC_{INF_obs} min*ng/mL	AUC_{%Extrap}	Cl_{obs} mL/min/kg	%F	Cl/%F
50mg/Kg IP Mouse-7	1.76	0.25	215	0.22	23638	0.40	31125	24.1	1606		28
50mg/Kg IP Mouse-8	3.99	0.25	165	0.17	21641	0.36	46569	53.5	1074		19
50mg/Kg IP Mouse-9	1.36	0.25	196	0.20	21436	0.36	25517	16.0	1959		34
Avg.	2.37	0.25	192	0.19	22238	0.37	34404	31.2	1547	0.02	27
Subject	T_{1/2} hr	T_{max} hr	C_{max} ng/mL	C_{max} μM	AUC_{last} min*ng/mL	AUC_{last} μM.hr	AUC_{INF_obs} min*ng/mL	AUC_{%Extrap}	Cl_{obs} mL/min/kg	%F	Cl/%F
10 mg/kg PO Mouse-7	2.35	0.08	166	0.17	27610	0.46	33153	16.7	302		38
10 mg/kg PO Mouse-8	1.55	0.25	137	0.14	23062	0.39	24984	7.7	400		51
10 mg/kg PO Mouse-9	2.74	1.00	185	0.19	45558	0.77	51524	11.6	194		25
Avg.	2.21	0.44	163	0.16	32077	0.54	36554	12.0	299	0.13	38
Subject	T_{1/2} hr	T_{max} hr	C_{max} ng/mL	C_{max} μM	AUC_{last} min*ng/mL	AUC_{last} μM.hr	AUC_{INF_obs} min*ng/mL	AUC_{%Extrap}	Cl_{obs} mL/min/kg	%F	Cl/%F
25mg/Kg PO Mouse-1	1.73	0.50	173	0.17	24479	0.41	26947	9.2	928		36
25mg/Kg PO Mouse-2	1.32	1.00	157	0.16	20637	0.35	24213	14.8	1032		40
25mg/Kg PO Mouse-3	0.95	0.50	223	0.23	28456	0.48	28768	1.1	869		34
Avg.	1.33	0.67	184	0.19	24524	0.41	26643	8.3	943	0.04	37
Subject	T_{1/2} hr	T_{max} hr	C_{max} ng/mL	C_{max} μM	AUC_{last} min*ng/mL	AUC_{last} μM.hr	AUC_{INF_obs} min*ng/mL	AUC_{%Extrap}	Cl_{obs} mL/min/kg	%F	Cl/%F
50mg/Kg PO Mouse-4	1.13	0.25	118	0.12	13205	0.22	14409	8.4	3470		53
50mg/Kg PO Mouse-5	3.90	1.00	113	0.11	25083	0.42	37645	33.4	1328		20
50mg/Kg PO Mouse-6	1.43	1.00	173	0.17	20061	0.34	24459	18.0	2044		31
Avg.	2.15	0.75	135	0.14	19450	0.33	25505	19.9	2281	0.02	35

Pharmacokinetics was assessed in C57Bl/6 mice with blood was collected at 0.08, 0.25, 0.5, 1, 2, 4, 6, and 8 hours. Plasma was generated by centrifugation and plasma concentrations were determined by LC-MS/MS following the mass transition 49600→340 AMU. Pharmacokinetic parameters were calculated using Phoenix WinNonlin® to determine peak plasma concentration (C_{max}), oral bioavailability (%F), exposure (AUC), half-life (t_{1/2}), clearance (CL), and volume of distribution (V_d). Compounds were formulated by dissolving into DMSO and then diluting with 10%

captisol (w:v) with the final formulation containing 5% DMSO. Dosed was by intraperitoneal injection, intravenous tail vein injection, or oral gavage. All procedures are approved by the Scripps Florida IACUC and Scripps vivarium is fully AAALAC accredited.

Table S4. Proteomics data for BTK degraders from Mino cells treated with 200 nM DD-03-171 or DD-04-118 for 4h.

Table S5. Patient and genetic information of PDX models. Extensive clinical, laboratory and genomic characterization of these PDX models can be found in the Public Repository of Xenografts (<http://www.PRoXe.org>)³. The Hemoseq platform of ~300 genes relevant to hematologic malignancies was published in Odejide et al. Blood 2014;123:1293-6.

	Cancer Type	Patient	Tumor mutations (variant allele fraction)	PDX mutations
DFBL-18689-V3	ABC-DLBCL	63 year-old white male presented with pancytopenia and hypercalcemia, found to have DLBCL. Sample obtained prior to first-line treatment	NOTCH2 NM_024408 c.7221_7221insTGAC p.H2408fs* - in 2.9% of 914 reads TET2 NM_001127208 c.4294_4301delGTGG AAGC p.S1431fs* - in 4.4% of 1457 reads DNMT3A NM_175629 c.1195C>T p.V399M - in 3.2% of 1603 reads NOTCH3 NM_000435 c.6134G>A p.P2045L - in 43.8% of 185 reads TET2 NM_001127208 c.100C>T p.L34F - in 52.9% of 499 reads	CARD11 Missense NM_032415 c.1267C>T p.R423W in 98.0% of 102 reads CCND3 Frameshift Insertion NM_001760 c.816_816C>GC p.G272fs in 48.5% of 101 reads
DFBL-39435-V2	MCL	67 year-old male with relapsed MCL after R-bendamustine and R maintenance then bortezomib	Sequencing not done. Del(17p) by FISH	TP53 Missense NM_001126112 c.469G>T p.V157F in 99.4% of 168 reads DNMT3A Missense NM_022552 c.2309C>T p.S770L in 44.6% of 314 reads MYC Missense NM_002467 c.176C>T p.A59V in 6.4% of 295 reads
DFBL-44685-V2	MCL	63 year-old male with relapsed MCL after autologous stem cell transplant, ibrutinib and TGR-1202.	ATM NM_000051 c.5014_5021delGGAA GCTG p.V1671fs* - in 40.5% of 237 reads	TP53 Missense NM_001126112 c.742C>T p.R248W in 86.7% of 180 reads

			<p>TP53 NM_000546 c.742G>A p.R248W - in 90.4% of 543 reads WHSC1 NM_133330 c.3295G>A p.E1099K - in 45.9% of 799 reads ATM NM_000051 c.7376G>C p.R2459P - in 52.0% of 3380 reads CREBBP NM_004380 c.6771C>A p.Q2257H - in 41.5% of 795 reads</p>	<p>CARD11 Missense NM_032415 c.688G>A p.D230N in 71.2% of 805 reads CREBBP Missense NM_004380 c.6771G>T p.Q2257H in 47.8% of 372 reads MLL3 Missense NM_170606 c.2959T>C p.Y987H in 30.4% of 621 reads MLL2 Nonsense NM_003482 c.646G>T p.E216* in 23.8% of 428 reads PRDM16 Missense NM_022114 c.352C>T p.R118W in 5.1% of 272 reads</p>
DFBL-96069-V2	MCL	<p>72 year-old Asian female with relapsed/refractory mantle cell lymphoma following several lines of chemotherapy (R-CHOP, COPDPL, FC, teniposide+cytarabine, cladribine, lenalidomide+dexamethasone). Ibrutinib was discontinued one month prior in the setting of thrombocytopenia and bilateral subdural hemorrhages. Refractory and intolerant to recent ibrutinib. Circulating disease (WBC 312600 with 61% atypical cells).</p>	Sequencing not done.	No mutations detected on ~300 gene Hemoseq platform.
DFBL-98848-mCLP-V4	MCL	<p>81 year-old white male with MCL relapsed after R-bendamustine</p>	<p>NOTCH1 NM_017617 c.7543_7544delAG p.P2514fs*4 - in 75.8% of 3099 reads KRAS NM_004985 c.408A>T p.S136R - in 7.8% of 141 reads</p>	No mutations detected on ~300 gene Hemoseq platform.

Supplementary Figures

Figure S1. Effects of BTK degradation on diffuse large B-cell lymphoma cells.

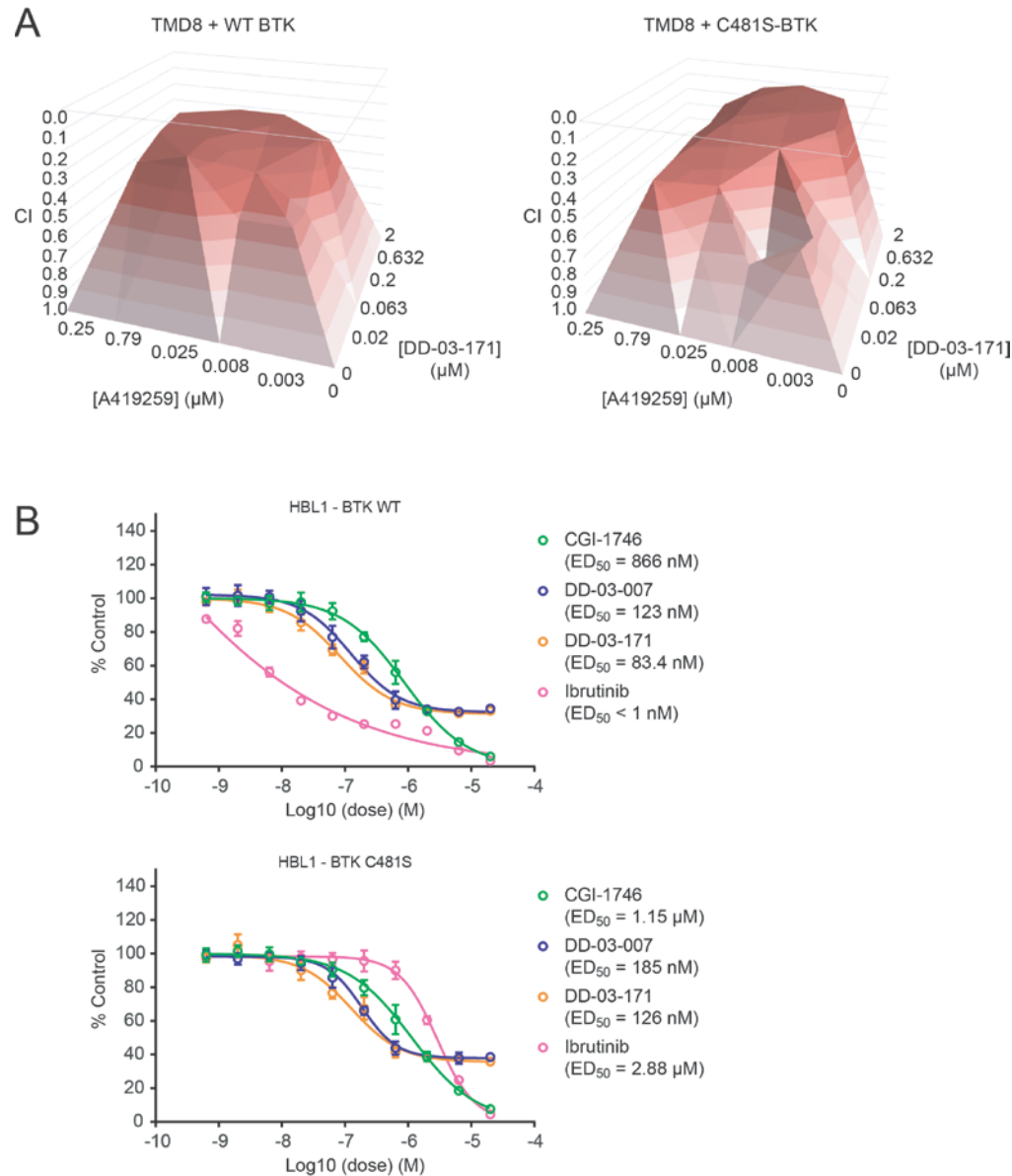


Figure S1. Effects of BTK degradation on diffuse large B-cell lymphoma cells.

(A) TMD8 cells expressing either WT- or C481S-BTK were treated with A419259 in combination with DD-03-171 for 3 days. Plots show combination index (CI) scores. CI < 1 indicates synergy. (B) Proliferation assays were performed by treating HBL1 DLBCL cells with compounds at the indicated concentrations for 72h. Anti-proliferative effects of compounds were assessed using Cell Titer Glo assay kit (Promega), and ED₅₀s were determined using Graphpad Prism nonlinear regression curve fit.

Figure S2. Combination study of BTK inhibitors and degraders in MCL cells.

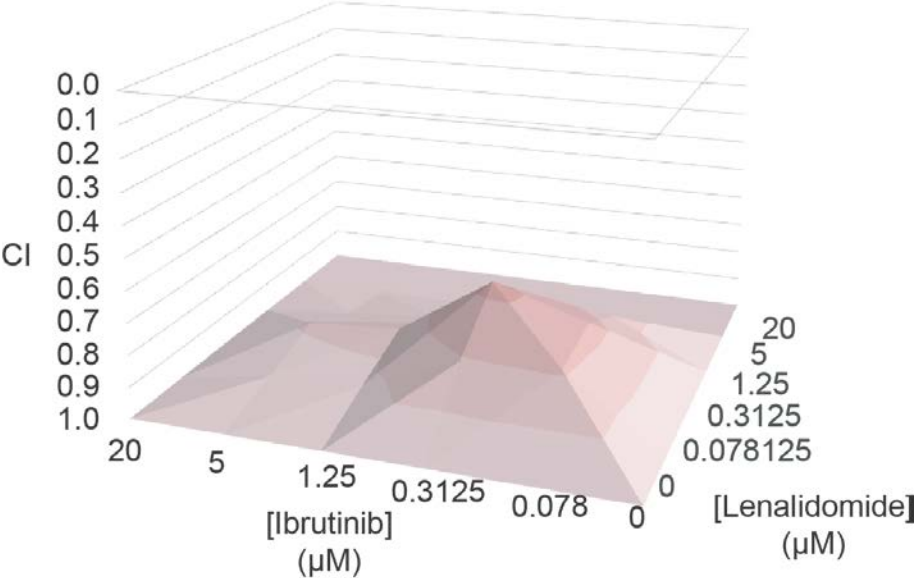


Figure S2. Combination study of BTK inhibitors and degraders in MCL cells. Mino cells were treated with ibrutinib in combination with lenalidomide, for 3d. Plots show combination index (CI) scores. CI < 1 indicates synergy.

Figure S3. Effect of BTK degradation on MCL cell proliferation.

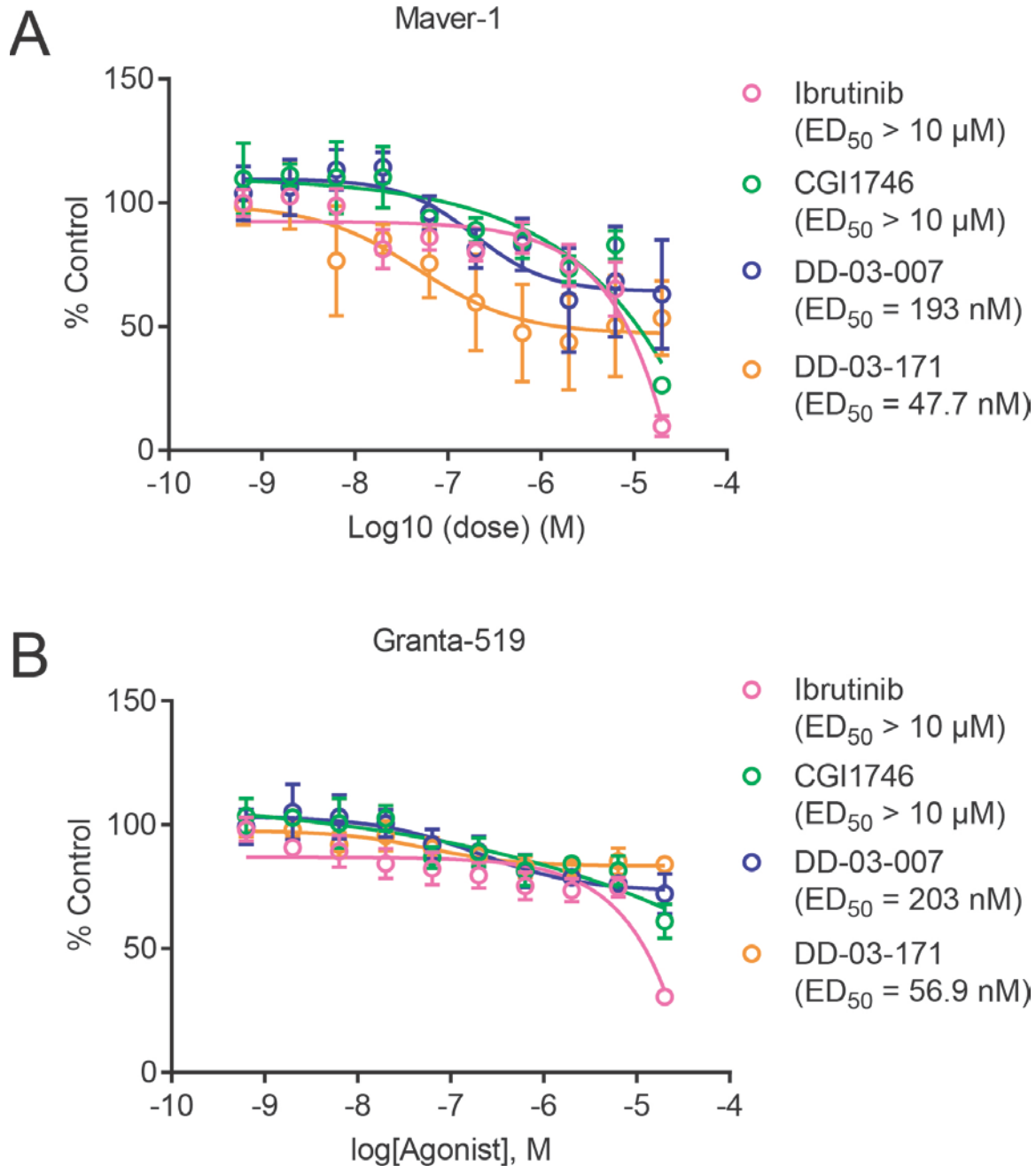


Figure S3. Effect of BTK degradation on MCL cell proliferation.

Proliferation assays were performed by treating **(A)** Maver-1 or **(B)** Granta-519 cells with compounds at the indicated concentrations for 72h. Anti-proliferative effects of compounds were assessed using Cell Titer Glo assay kit (Promega), and ED_{50} s were determined using Graphpad Prism nonlinear regression curve fit.

Figure S4. Effects of BTK degradation on NFκB signaling.

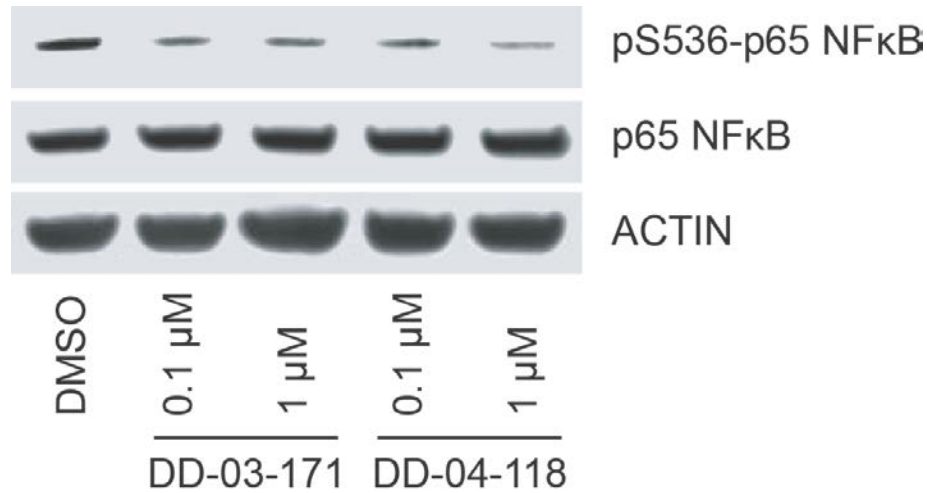


Figure S4. Effects of BTK degradation on NFκB signaling. Immunoblots from Mino cells treated with the indicated compounds for 18h.

Figure S5. *In vivo* degradation efficacy of BTK degraders.

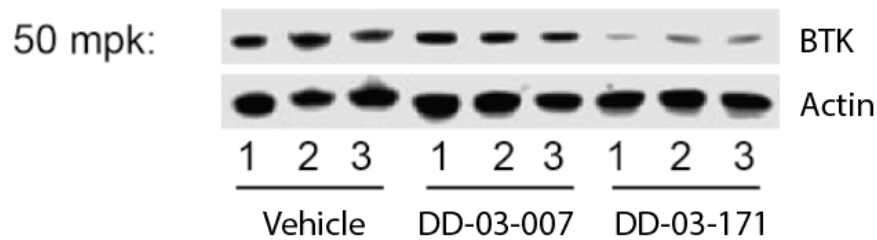


Figure S5. *In vivo* degradation efficacy of BTK degraders. Healthy C57BL/6 mice were treated with indicated compounds for 3 days, BID, via intraperitoneal (IP) injection. Mouse spleens (RBC-depleted) were collected 6h after the last injection and immunoblotted for BTK. Each lane represents an individual mouse (3 per treatment cohort).

Figure S6. Effects of BTK degradation on DFBL-18689 *in vivo*.

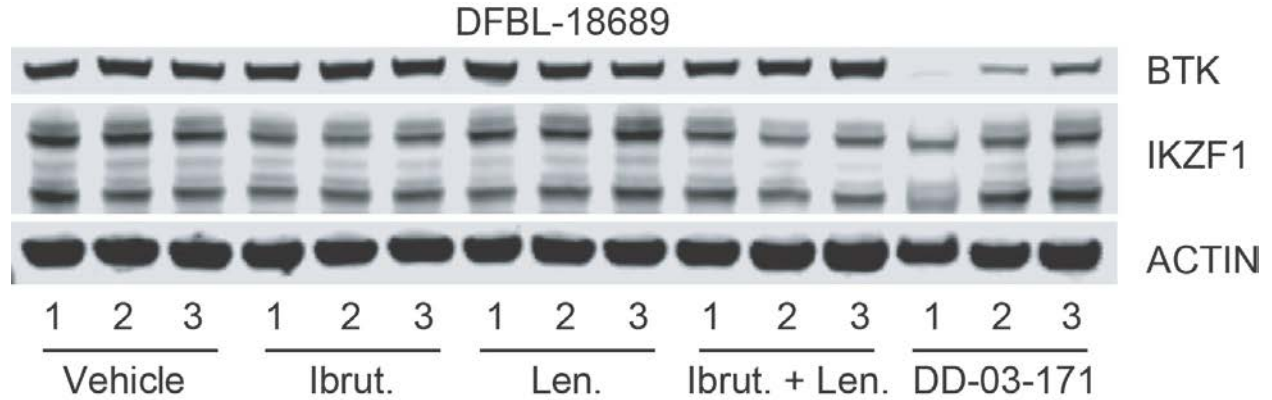


Figure S6. Effects of BTK degradation on DFBL-18689 *in vivo*.

NSG mice were engrafted with DFBL-18689 cells (derived from a patient with DLBCL). Immunoblots from mouse-depleted spleen samples of individual mice collected at endpoint treated as indicated: vehicle (IP, BID), ibrutinib (PO, QD, 30 mg/kg), lenalidomide (IP, QD, 50 mg/kg), lenalidomide + ibrutinib, or DD-03-171 (IP, QD, 50 mg/kg). Percent circulating disease (CD20+/CD19+)

Figure S7. Effects of BTK degradation on DFBL-39435 *in vivo*.

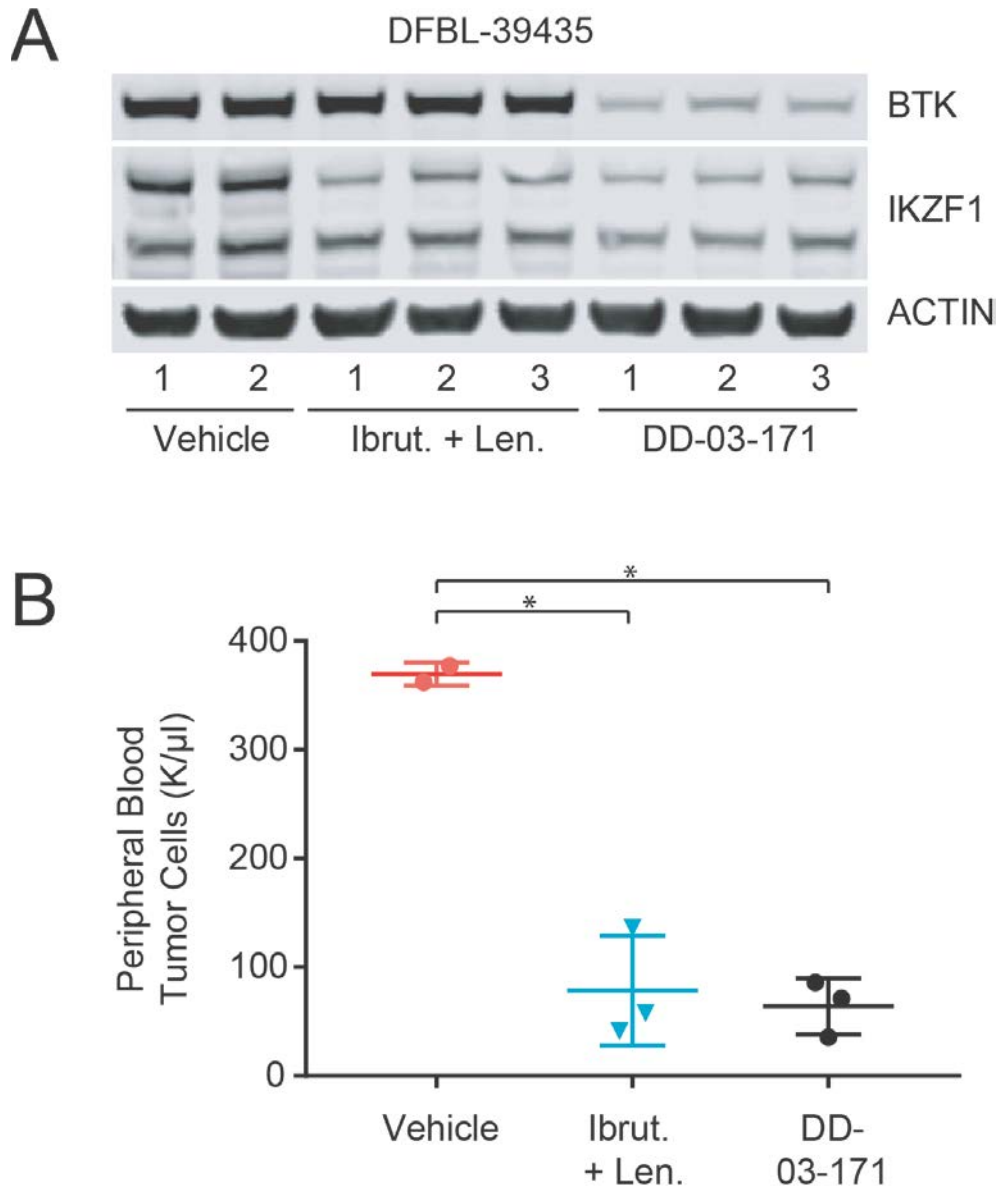


Figure S7. Effects of BTK degradation on DFBL-39435 *in vivo*.

NSG mice were engrafted with DFBL-39435 cells (derived from a patient with MCL). **(A)** Immunoblots from mouse-depleted spleen samples of individual mice collected after 3d treatment with indicated: vehicle (IP, BID; n=2), ibrutinib (PO, QD, 30 mg/kg) + lenalidomide (IP, QD, 50 mg/kg) (n=3), or DD-03-171 (IP, QD, 50 mg/kg; n=3). **(B)** Peripheral tumor blood burden after 14d treatment. * $p < 0.05$.

Figure S8. Effects of BTK degradation on DFBL-44685 *in vivo*.

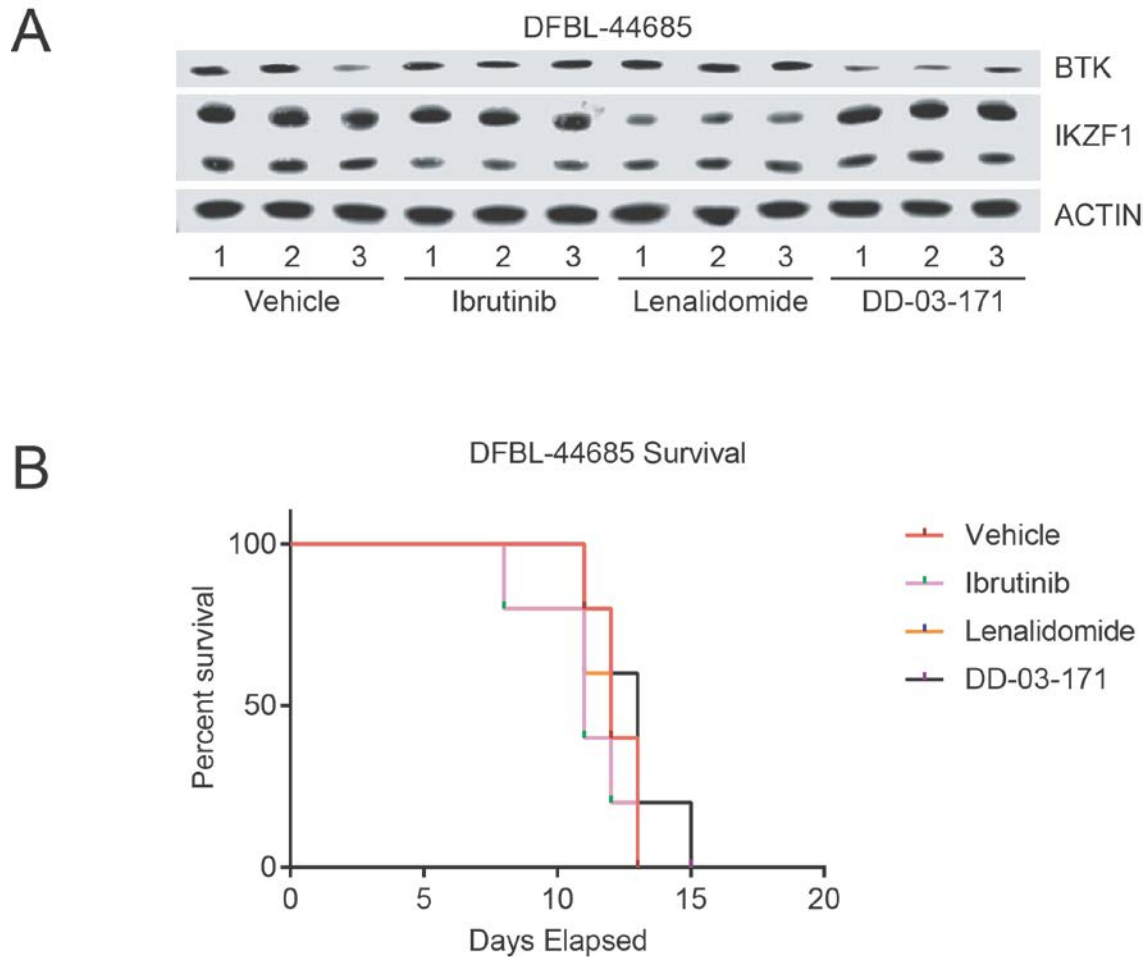


Figure S8. Effects of BTK degradation on DFBL-44685 *in vivo*.

NSG mice were engrafted with DFBL-44685 cells (derived from a patient with MCL). **(A)** Immunoblots from mouse-depleted spleen samples of individual mice collected after 3d treatment with indicated: vehicle (IP, BID), ibrutinib (PO, QD, 30 mg/kg), lenalidomide (IP, QD, 50 mg/kg), or DD-03-171 (IP, QD, 50 mg/kg). **(B)** Survival of xenografted NSG mice as treated in (A). n=5 for each cohort.

Figure S9. Effects of BTK degradation on DFBL-98848 *in vivo*.

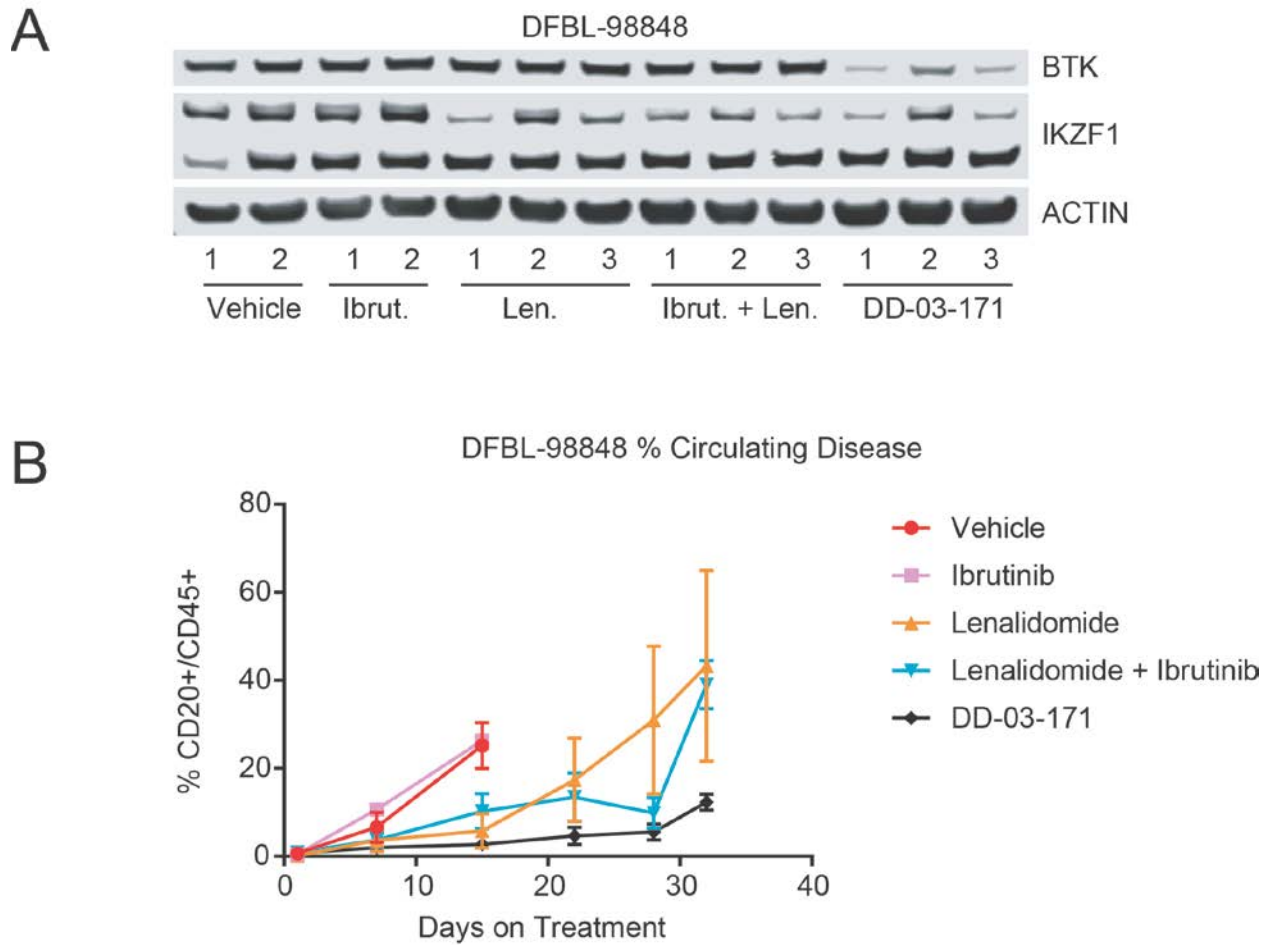


Figure S9. Effects of BTK degradation on DFBL-98848 *in vivo*.

NSG mice were engrafted with DFBL-98848 cells (derived from a patient with MCL). **(A)** Immunoblots from mouse-depleted spleen samples of individual mice collected at endpoint treated with indicated: vehicle (IP, BID), ibrutinib (PO, QD, 30 mg/kg), lenalidomide (IP, QD, 50 mg/kg), lenalidomide + ibrutinib, or DD-03-171 (IP, QD, 50 mg/kg). **(B)** Percent circulating disease of xenografted NSG mice as treated in (A). vehicle (n=2), ibrutinib (n=1), lenalidomide (n=2), lenalidomide + ibrutinib (n=3), or DD-03-171 (n=3).

References

1. An J, Ponthier CM, Sack R, et al. pSILAC mass spectrometry reveals ZFP91 as IMiD-dependent substrate of the CRL4(CRBN) ubiquitin ligase. *Nat Commun.* 2017;8:15398.
2. McAlister GC, Nusinow DP, Jedrychowski MP, et al. MultiNotch MS3 enables accurate, sensitive, and multiplexed detection of differential expression across cancer cell line proteomes. *Anal Chem.* 2014;86(14):7150-7158.
3. Townsend EC, Murakami MA, Christodoulou A, et al. The Public Repository of Xenografts Enables Discovery and Randomized Phase II-like Trials in Mice. *Cancer Cell.* 2016;29(4):574-586.